THE JOURNAL OF PHYSICAL CHEMISTRY B

Article

pubs.acs.org/JPCB

Interionic Hydration Structures of NaCl in Aqueous Solution: A Combined Study of Quantum Mechanical Cluster Calculations and QM/EFP-MD Simulations

Manik K. Ghosh,[†] Suyong Re,[‡] Michael Feig,[§] Yuji Sugita,*[,‡] and Cheol Ho Choi*[,†]

[†]Department of Chemistry and Green-Nano Materials Research Center, College of Natural Sciences, Kyungpook National University, Taegu 702-701, Korea

[‡]RIKEN Advanced Science Institute, 2-1 Hirosawa, Wako, Saitama 351-0198, Japan

[§]Chemistry and Biochemistry & Molecular Biology, Michigan State University, East Lansing, Michigan 48824, United States

Supporting Information

ABSTRACT: The association process of NaCl in aqueous solution was studied by a combination of quantum mechanical calculations on $NaCl(H_2O)_n$ (n = 1−6) clusters and quantum mechanical/effective fragment potential−molecular dynamics (QM/EFP-MD) simulations for NaCl in 292 EFP waters. The interionic hydration structures (IHSs) were topologically classified as "ring" (R), "half-bridge" (H), and "full-bridge" (F) types on the basis of the quantum mechanical calculations. Subsequent IHS analysis on QM/EFP-MD simulations revealed that the NaCl contact ion pair (CIP) mainly involved R type hydration structures while the solvent-separated ion pair (SSIP) was composed of two different groups of F-type hydration structures. Our IHS analysis also discovered H type hydration even at large separation interionic distances (∼7 Å), which is denoted as a dissociating ion pair (DIP). The analysis was able to reveal the most complete interionic structures and their reorganizations of the association process. A strong correlation between the IHSs and interionic distance suggests that not only the solvent reorganization but also the local IHS changes are equally important. Mechanistically, it is suggested that the conversion between ring-type and full-bridge hydration structures is the main rate-determining step of ion-pair association.

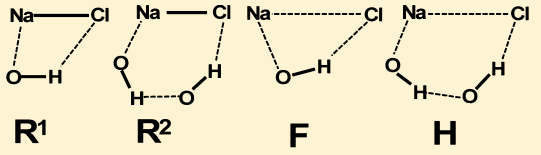

IHS(Interionic Hydration Structures)

1. INTRODUCTION

The association of opposite ions to form a unique entity in solution has an important role in chemical reactions,[1−3] solvation of ionic crystals into water,[4] functionality of biological systems,[5−9] and even functionality of aerosols in atmosphere.[10−13] The general scheme for the association reaction of two ionic solutes may be written as

$$M^+_{ions} + X^- \Leftrightarrow M\cdots X_{SSIP} \Leftrightarrow M\cdot X_{CIP} \Leftrightarrow MX_{salt}$$

where the reaction involves two intermediates, the contact ion pair (CIP) and the solvent separated ion pair (SSIP). No solvent molecules intervene between the ions in CIP, while the two ions are held apart by solvent in SSIP. These intermediates were first proposed by Winstein et al.[14] Early attempts with primitive continuum models and experiments of electrolyte conductance[15−18] established that all electrolytes in dilute aqueous solutions have a general trend to associate or even form stable neutral ion pairs,[19] which is prominently regulated by the dielectric constant of the solvent. Since oppositely charged ions in solutions are generally attracted by the Coulombic interaction, the magnitude of charge and radius of ions are important for the ion association. On the other hand, entropy generally opposes the ion association.

The structure and stability of these ion pairs have been extensively studied using quantum mechanical calculations on model clusters. The stable structures of $NaCl(H_2O)_n$[20−29] clusters have been well characterized at various levels of quantum theories. Woon and Dunning[20] showed that the most stable structure of NaCl−H_2O has a four-membered ring conformation. They pointed out that the interionic distance of NaCl lengthens with an increasing number of H_2O molecules. Similar results were independently derived by Asada and Nishimoto[21] from Monte Carlo simulations for $NaCl(H_2O)_n$ (n = 1−8). Petersen and Gordon[22] investigated $NaCl(H_2O)_n$ ($n \leq$ 10) clusters using the effective fragment potential (EFP) and showed that Na^+ and Cl^- are in close contact even with 10 water molecules. On the contrary, Jungwirth[23] predicted that 6 water molecules dissociate the NaCl into SSIP with the interionic distance of 4.43 Å based on accurate quantum chemical calculations. With the help of *ab initio* molecular dynamics, Siu et al.[30] found a new CIP structure, in which the NaCl pair interacts with three independent H_2O dimers instead of the two three-membered H_2O rings that were found by Jungwirth. They also showed that the relative stability between

Received: September 3, 2012
Revised: November 30, 2012
Published: December 11, 2012

CIP and SSIP depends both on the cluster size (the number of water molecules) and on entropy (temperature). In general, these cluster calculations commonly found that the successive addition of water molecules to the cluster increases the alkali metal−halide distances. Although the cluster calculations provide accurate energies and structures, the adopted models are not sufficiently large to represent the hydration structures in solution.

Various molecular dynamics (MD) simulations were used to study the thermodynamics and kinetics of M−Cl (M = Li, Na, and K) in solution.[31−45] The calculated potentials of mean force (PMFs) for ion associations commonly show the CIP and SSIP minima for LiCl, NaCl, and KCl. Using classical MD simulations, Smith and Dang[31] estimated the CIP and SSIP interionic distances of NaCl as 2.8−2.9 Å and ∼5 Å, respectively. However, recent *ab initio* MD (AIMD) simulations on NaCl[46] reported a remarkable difference in the free energy profiles between the *ab initio* and classical PMFs. The *ab initio* PMF shows a shallower CIP minimum and a smaller transition barrier toward the SSIP as compared to the classical profiles. They also showed that the current classical models tend to overcoordinate the ion pair at all distances, giving a rather deep minimum for the CIP. Although the general ion association features for CIP and SSIP of metal−halide PMFs are now well captured by MD simulations, the local hydration structures of ion pairs in solution still remain unclear.

Previous MD studies suggest[47] that simulations for 100−200 ps are necessary to obtain converged hydration dynamics. Although AIMD simulations such as CPMD[48] or FMO-MD[49] can provide the most direct tool for studying ion association, AIMD simulations over such time scales for systems with sufficient size are still difficult. To overcome this challenge, the quantum mechanical/molecular mechanical (QM/MM) method is often utilized.[50] As an alternative and more preferable approach, the classical MM force field can be replaced with a quantum mechanically driven force field. One such model is based on a fragment-based potential, known as EFP (effective fragment potential),[51] that was proposed by Gordon and coworkers. In the EFP approach, each water molecule is represented as a fragment of fixed geometry with a set of parameters deduced from *ab initio* calculations. In the original implementation,[52] called EFP1, the interaction energy between water molecules consists of Coulomb, polarization, and repulsion terms. The Coulomb term is evaluated using classical multipoles up to octupoles that are centered at each atom and at bond midpoints. The fragment polarization energy is evaluated by considering the interaction of induced dipoles of each fragment with the static field due to the Coulomb multipoles as well as the induced field due to the induced dipoles of the other fragments. The induced dipoles are located at the centroids of localized molecular orbitals (LMO) at which (anisotropic) distributed polarizability tensors are placed. The remaining contribution to the *ab initio*−EFP interactions accounts for exchange-repulsion and charge transfer effects, which is modeled in the form of Gaussian functions. The hybrid QM/EFP method has been successfully applied to the water structures,[53,54] chemical reactions,[55,56] and photochemistry in water.[57] It was shown that the EFP could successfully reproduce full QM results with comparatively low computational cost.[51] Therefore, one clear advantage of EFP as compared to classical parameters is its chemical accuracy in the calculations of energies and structures. The applicability of the hybrid QM/EFP to a long-time MD simulation of chemical reaction in aqueous solution has been recently examined,[58] where it was found that the QM/EFP-MD yields accurate free energy change and barrier associated with the transition from the zwitterion to nonionized form of glycine in aqueous solution. This also demonstrated that sampling on the order of ∼100 ps is sufficient to properly describe the local hydrogen bonding dynamics.

As discussed earlier, quantum mechanical cluster calculations can provide accurate static structures of microsolvated structures, while MD yields the averaged dynamic aspects of solvation. In the present work, we perform both quantum mechanical cluster calculations and QM/EFP-MD simulations on the NaCl ion pair in aqueous solution in order to obtain the structural feature of NaCl association and dissociation. We first extracted the local structural motifs of interionic hydration structures (IHSs) from accurate quantum mechanical calculations. Then, they were subsequently utilized for the characterizations of the hydration structures and the related association mechanism of NaCl in aqueous solution.

2. COMPUTATIONAL DETAILS

Full geometry optimizations were performed on $NaCl(H_2O)_n$ (n = 1−6) clusters. The gradient correlated density functional theory (DFT) with Becke three-parameter exchange function[59] and the Lee−Yang−Parr correlation function[60] (B3LYP) in combination with all-electron 6-311++G(d,p)[61] basis set were adopted. The convergence criteria of geometry optimizations are 0.0001 hartree/Bohr.

A spherical system of a single NaCl molecule solvated with 292 water molecules was prepared for the QM/EFP-MD simulations. The NaCl pair and waters are treated with HF/6-31G(d) and EFP1, respectively. In order to prevent evaporation of waters during long time simulations, we applied a harmonic restraint potential for the boundary solvent molecules as implemented in CHARMM.[62] Umbrella sampling along the ion−ion distance reaction coordinate was carried out. Eight windows were prepared covering distances from 2.0 to 9.0 Å with a spacing of 1.0 Å. The potentials of mean force (PMFs) between the two ion pairs from the umbrella windows were obtained using the weighted histogram analysis method (WHAM).[63] The main idea of WHAM consists of constructing an optimal estimate of the unbiased distribution function as a weighted sum over the data extracted from all the simulations and of determining the functional form of the weighted factors that minimize the statistical error. Initially, NVT runs of QM/EFP-MD simulations over 50 ps were performed on each of the eight windows at 300 K to equilibrate the systems. Then, QM/EFP-MD production runs, also in the NVT ensemble and at 300K, were continued for 150 ps from the final structures after the equilibration. The statistical error of our simulations was estimated by the square of cumulative statistical error as suggested by Zhu and Hummer.[64] The estimated square of cumulative error in our calculated free energy is 0.0805 kcal/mol, which is a good indication of converted PMF. All calculations were performed with a modified version of GAMESS.[65] Our implementation is currently available in the most recent version of GAMESS.

Scheme 1 shows the basic types of interionic hydration structure (IHS) that were found in our quantum mechanical calculations on clusters. The R^1, R^2, F, and H represent one-water "ring", two-water "ring", "full-bridge", and "half-bridge" structures, respectively. The recognition of IHS motifs was

dx.doi.org/10.1021/jp308731z | J. Phys. Chem. B 2013, 117, 289−295

Scheme 1. The Basic Topologies of Interionic Hydration Structures (IHSs)

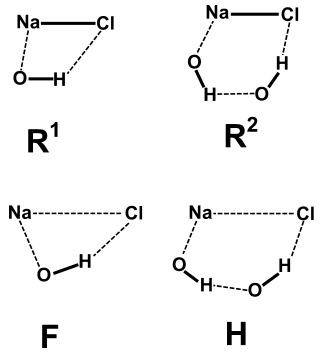

entirely based on the ion−water and water−water interactions. For example, if a water molecule interacts with Na^+ and Cl^- at the same time, the structure is recognized as R^1 or F, depending on Na−Cl interionic distance. A distance criterion for the interaction is set to be 2.8 Å, which is a typical hydrogen bond distance. Since the R^1 and F types will naturally appear in the histogram, no additional classification between the R^1 and F is necessary. Likewise if two water molecules form a hydrogen bond with each other and at the same time interact with Na^+ and Cl^- as shown in Scheme 1, the structure is recognized as R^2 or H. In other words, the Na and Cl are connected by a bridge, which is composed of two water molecules. The Na−Cl interionic distance is critical to distinguish the "ring" and "bridge" (full-bridge, F, or half-bridge, H) structures. The R^1 and R^2 become F and H, respectively, as the r(Na−Cl) increases. This structural classification was applied to all of the fully optimized $NaCl(H_2O)_n$ clusters.

3. RESULTS AND DISCUSSION

A. Interionic Structural Classifications of Model Clusters. We performed full geometry optimizations on the model clusters of $NaCl(H_2O)_n$ (n = 1−6) at the B3LYP/6-311++G(d,p) level in order to identify the general structural motifs of interionic hydration structures (IHSs) of NaCl ion pairs. All of the optimized structures are shown in Figure 1. (Detailed figures can be found in Figure S1 of the Supporting Information.) The stabilization energy (ΔE) of each cluster was calculated by subtracting energies of NaCl (E(NaCl)) and water molecules ($nE(H_2O)$) from the energy of the respective cluster ($E(NaCl(H_2O)_n)$). Our results are, in many aspects, consistent with previous reports from different theoretical groups.[20,22,29] The optimized structures were classified using four types of structural motifs, R^1, R^2, F, and H, as shown in Scheme 1 (see more details in Computational Details). In short, R represents a contact Na^+Cl^- pair forming a cyclic hydrogen bond with water molecule. The superscript and subscript in R denote the number of water molecules involved in the ring and the number of rings, respectively. F and H represent a dissociated Na^+Cl^- pair bridged by one and two water molecules, respectively. The R^1 and R^2 configurations become F and H when r(Na−Cl) increases. For example, the structure **2b** in Figure 1 is represented by R^2_1, meaning that it has one ring structure composed of two water molecules. Likewise, the R^1_3 is used to represent the structures **3a**, **4c**, and **4d** that commonly possess three ring structures involving a single water molecule. The r(Na−Cl) of R structures are

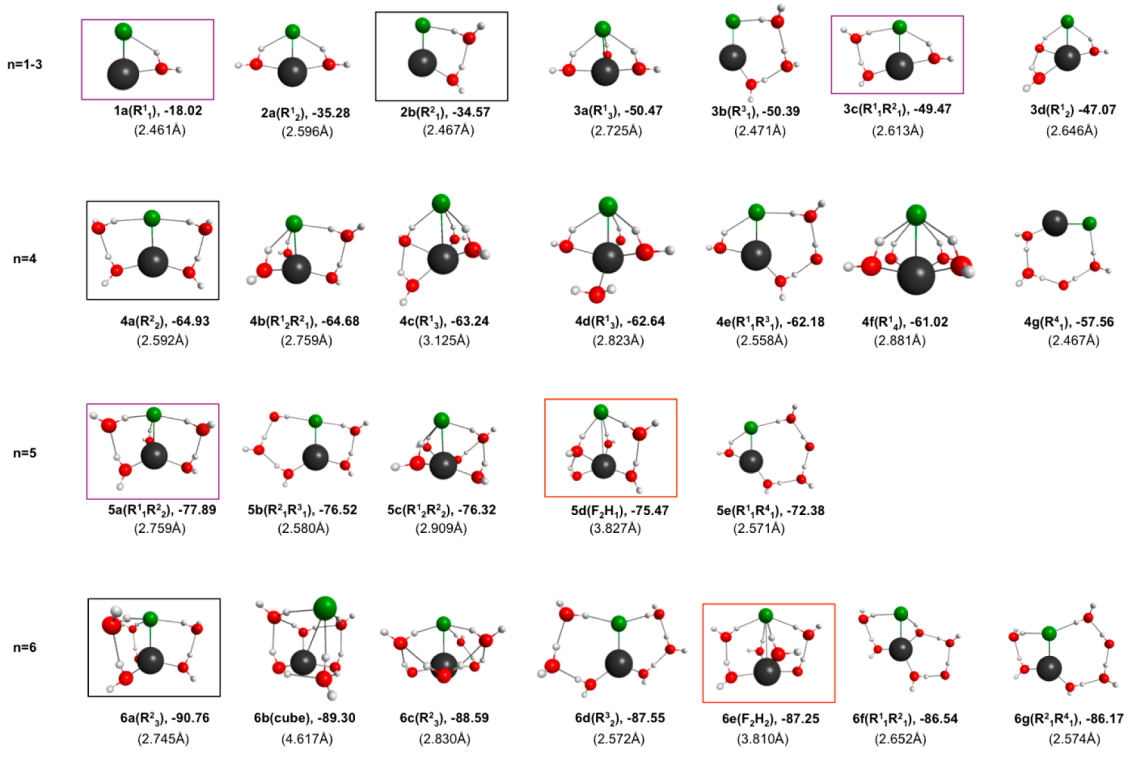

Figure 1. Optimized structures and stabilization energies of $NaCl(H_2O)_n$ (n = 1−6) clusters obtained from DFT calculations at the B3LYP/6-311++G(d,p). Detail structures are presented in the Supporting Information. The NaCl distances and energies are in Å and kcal/mol, respectively. The structures in boxes correspond to the interionic hydration structures found in our QM/EFP simulations (Figure 3). The color of boxes corresponds to those in Figure 3.

dx.doi.org/10.1021/jp308731z | J. Phys. Chem. B 2013, 117, 289−295

generally in the range of 2.46−3.13 Å. The contact pair structures having R type are the most stable for all cluster sizes examined (**1a**−**6a**). Except for the R^1 structure of **1a** with one water (n = 1), the most stable structures of n = 2−6 consist of R^2, where two water molecules are forming a ring with NaCl. It indicates that R^2 is energetically favored. The first "bridge structure" appears at n = 5 (**5d**), which is 2.4 kcal/mol less stable than the most stable contact pair structure (**5a**). Additional bridge structures were found at n = 6 (**6b** and **6e**). The two-bridge structures, **5d** and **6e**, are represented by a combination of F and H forms, F_2H_1 and F_2H_2, respectively. For example, F_2H_1 implies that there are two one-water bridges (F) and one two-water bridge (H). The r(Na−Cl) of these structures is about 3.8 Å, which is 1 Å shorter than the typical value of SSIP found in MD simulations. The structure **6b** (r(Na−Cl) = 4.6 Å) closely resembles what was found by Siu et al. and Jungwirth et al. previously, where Na^+ and Cl^- are separated by a cyclic hydrogen-bonded water hexamer. However, this cubelike structure may not be the major species in solution due to the large entropy cost to form such a highly compact and ordered structure.

The stability of R structures generally results from the direct bonding interaction between Na and Cl. Therefore, it can be expected that their structures are less influenced by solvation. In contrast, the stability of bridge structures comes from the bonding interactions of Na−O and Cl−H, and partially from the Coulombic attractions between Na and Cl. Therefore it can be expected that the bridge structures are more affected by solvation effects. It should be emphasized that all of the structures can be classified by our IHS scheme, indicating that IHS is a useful way of characterizing NaCl hydration structures.

B. PMF of NaCl Association Process in Solution. The potential of mean force (PMF) along the NaCl interionic distance obtained from the QM/EFP-MD simulations is presented in Figure 2a. PMFs from previous simulations are also shown for comparison (data taken from ref 46). Our PMF profile closely resembles the CPMD result (Figure 2a).[46] The CPMD simulations were carried out for 6 ps while keeping the reaction coordinate of NaCl distance fixed. Both QM/EFP-MD and CPMD show a shallower CIP minimum and a smaller transition barrier toward the SSIP as compared to the classical profiles. We also note that the positions of minima as well as the transition states (TS) connecting them are slightly shifted toward the longer side in our PMF compared with the CPMD PMF. There are some possible sources for the difference. First, CPMD simulation was performed on a cubic box of 12.5 Å length with 64 water molecules corresponding to an ∼0.9 M salt solution, while our spherical system with 11 Å radius yields an ∼0.3 M solution. This nominal difference in the concentration may affect the resulting PMF.[66] Further studies with various concentrations would be desirable. But, there are issues with reaching higher concentrations. Reducing the box size may introduce finite size and periodic boundary artifacts. On the other hand, including additional multiple ion pairs would greatly increase sampling demands beyond what is currently feasible with the QM/EFP-MD approach. However, the concentration dependence on the PMFs reported here is an important point that merits further investigation in a future study. Second, CPMD uses a density functional theory, while our calculations were performed at the HF level. The difference in the theory may also impact the PMF.[46] Among the classical simulations, the PMF by Smith and Dang appears to be the closest to our QM/EFP-MD, which can be attributed to their polarizable force field.

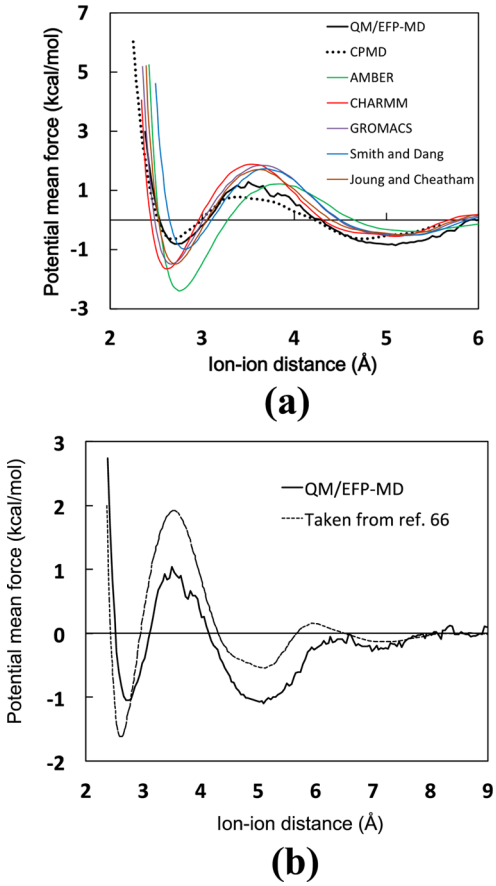

Figure 2. (a) Comparison of the QM/EFP (HF/6-31G(d) for QM) PMF for dissociation of NaCl with the *ab initio* (CPMD) and the classical MD. The PMFs of CPMD, AMBER, CHARMM, and GROMACS were taken from ref 46. The PMFs of Smith and Dang and Joung and Cheatham were taken from refs 31 and 38. The calculations were done by CHARMM (version 27), AMBER (version 9), and GROMACS (version 3) force fields as well as the parameters determined by Smith and Dang[31] and Joung and Cheatham[38] (b) QM/EFP-MD and classical MD[66] PMFs for dissociation of NaCl.

Experimentally, the solubility limit of aqueous NaCl at room temperature is 5.4 M.[67] Thus, no clustering of opposite ions should occur for the dilute solutions as Timko et al. argued.[46] The binding free energy is very small in absolute value in both QM/EFP-MD and CPMD cases, which more or less ensures this. The concentrations at which the ion−ion interactions become relevant have been studied by Aragones et al.[68] using three different classical force fields. They found that the predictions of the solubility are quite sensitive to the details of the force field used.

QM/EFP-MD PMF is characterized by three minima at 2.7, 5.1, and 7.0 Å in Figure 2b, where the interionic distance is shown up to 9.0 Å. The first and second minima correspond to the CIP and SSIP, respectively. A very shallow minimum with 0.3 kcal/mol binding energy appears around r = 7 Å. Such a minimum is also seen in the classical MD simulations,[66,68] but no attention has been paid in past studies. Since its minimum position is at a nearly dissociating distance of Na−Cl, we denote the minimum as dissociating ion pair (DIP). The third minimum is very shallow but may play a role as an intermediate in the ion association process in solution.

dx.doi.org/10.1021/jp308731z | J. Phys. Chem. B 2013, 117, 289−295

To make better connections with experiments, the association constant (K_a) of Na^+Cl^- and the equilibrium constant (K_e) between SSIP and CIP were calculated using our PMF. The formula of the equilibrium and association constants at infinite dilution was taken from Chialvo et al.,[69] and the results are presented in Table 1. The values from Chialvo et al.

Table 1. Calculated Association and Equilibrium Constants[a]

model	log K_a	log K_e	R_L (Å)	R_U (Å)
QM/EFP-MD	4.86	1.17	3.5	9.0
PRH	4.36	−0.84	4.5	8.1
PR	4.03	−0.38	3.9	8.1
CHJ	3.71	0.08	3.7	8.1

[a]The values of PRH, PR, and CHJ were taken from ref 68.

were obtained at the critical water condition (the system density and temperature of 0.27 g/cm^3 and 616 K). On the other hand, our simulations were done at 0.99 g/cm^3 and 298 K. The radial distribution function of Na−Cl pair (g_{NaCl}) was obtained from the PMF according to $W(r) = -kT \ln g_{NaCl}(r)$ and is presented in the Supporting Information as Figure S2. Then, the association constant (K_a) can be calculated by

$$K_a = 4\pi \int_{R_L}^{R_U} g_{NaCl}(r) r^2 \, dr \quad (1)$$

where the R_L and R_U denote the lower and upper radial bounds for the solvation shell. Likewise, the equilibrium constant (K_e) of [SSIP]/[CIP] becomes

$$K_e = \int_{R_L}^{R_U} g_{NaCl}(r) r^2 \, dr \Big/ \int_{0}^{R_L} g_{NaCl}(r) r^2 \, dr \quad (2)$$

Our predicted K_a = 4.86 is larger than the previously reported values for higher temperatures. It is expected that the association constant becomes larger at lower temperatures. Therefore our prediction is consistent with previous findings. The predicted K_e = 1.17 is much larger than previous values, indicating that the SSIP and CIP are nearly equal concentrations. The larger K_e found in our study can be attributed to the differences in temperatures. This value can also be affected by the simulation methods. As seen in Figure 2, the classical parameters tend to underestimate the relative free energy of SSIP as compared to CIP, which yielded a smaller K_e.

C. Characterization of Association by IHS. All snapshots of the QM/EFP-MD simulations were analyzed in search of interionic hydration structures (IHSs). The analysis was performed on all of the umbrella sampling windows. The recognition of IHS motifs was only based on the hydrogen bond connectivity. For example, if a water molecule is forming hydrogen bonds of O−Na and H−Cl at the same time, the structure is recognized as R^1 or F. A maximum hydrogen bond distance of 2.8 Å was used to recognize its connectivity. The difference between R^1 and F comes from the interionic distance. Since the R^1 and F types will naturally appear in the histogram, no additional classification is necessary. Likewise if two water molecules are forming a hydrogen bond with each other and at the same time forming O−Na and H−Cl as shown in Scheme 1, the structure is recognized as R^2 or H. The results of our structural analysis are summarized in Figure 3 and Table 2. The IHSs in CIP region are characterized by various R structures. Note that we classify them as R, since they appear around 2.7 Å. The major species are R^2 type of R^2_1, R^2_2, and R^2_3

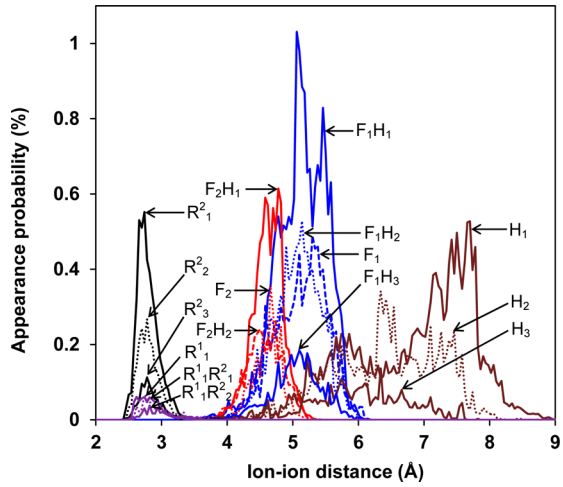

Figure 3. Distribution of the interionic hydration structures (IHSs) found in QM/EFP (HF/6-31G(d) for QM) MD runs. The appearance probability was weighted by WHAM (weighted histogram analysis method). The numbers are represented in percentage scale. The R^1, R^2, F_2, F_1, and H groups are represented in purple, black, red, blue, and brown colors, respectively.

Table 2. The relative Populations of Interionic Hydration Structures (IHSs)

type of structures		probability (%)
R		
	R^2_1	4.608
	R^2_2	2.365
	R^2_3	0.905
	R^1_1	0.681
	$R^1_1R^2_1$	0.628
	$R^1_1R^2_2$	0.357
F1		
	F_1H_1	18.762
	F_1H_2	10.461
	F_1	10.292
	F_1H_3	3.533
F2		
	F_2H_1	7.917
	F_2	4.125
	F_2H_2	3.162
H		
	H_1	17.626
	H_2	10.981
	H_3	3.598

in descending order, where the Na^+−Cl^- pair forms a cyclic hydrogen bond with two water molecules. The minor species involve R^1 types, in which single water molecule participates in the cyclic hydrogen bond, and the mixed form of R^1R^2 types. The preference of R^2 type was also seen in our cluster calculations. These coincidences imply that the major species of R group is determined by enthalpic stabilization. In general, IHS with a smaller number of rings is populated more than those having multiple rings. The peak for each R type is around 2.7 Å, which corresponds well with the values of R types found in quantum mechanical calculations (2.46−3.13 Å, see section A). The previous AIMD simulations of model clusters[30] reported that r(Na−Cl) of CIP is essentially independent of cluster size, consistent with our findings.

dx.doi.org/10.1021/jp308731z | J. Phys. Chem. B 2013, 117, 289−295

In contrast to the CIP, two groups (red and blue) with maximum positions of 4.7 and 5.3 Å appear near the SSIP interionic distance. They can be characterized as F_2 and F_1 species, since their maximum positions are mostly determined by the number of F rather than H hydration patterns. According to our classifications, the red peaks are F_2H_1, F_2, and F_2H_2 species in descending populations, while the blue ones are F_1H_1, F_1H_2, F_1, and F_1H_3. (See also Table 2.) The F type of IHS has one water molecule inserted into the NaCl bond as shown in Scheme 1. The F_2 and F_1 are the structures having two F types and one F type, respectively. The F_1 type IHS structure was not found in our cluster calculations (Figure 1). Only F_2 structures with 5 and 6 water clusters were found as stable species. In solution, the less rigid F_1 structures are likely favored due to entropic factors. The center position of F_2 is 4.7 Å, which is longer than the corresponding r(Na−Cl) of 3.8 Å found in the quantum mechanical cluster calculations. This difference suggests that long-range solvation contributions significantly affect the r(Na−Cl) of SSIP as well as the relative population of F groups in solution, which is different than the case of CIP. To the best of our knowledge, the existence of two SSIP groups has not been suggested before.

The third shallow minimum, dissociating ion pair (DIP), is characterized by H species, where a hydrogen bond chain involving two water molecules holds Na^+ and Cl^- at the same time. The H type of structures covers a wide range of r(Na−Cl) from 4 to 9 Å. The three types of H_1, H_2, and H_3 correlate well with the interionic distance. As such, the peak position shifts from 7.5 Å to 6.5 Å as the number of H bridges increases. The H_1 and H_2 types correspond to the DIP minimum (7 Å) of the PMF. The pure H type structures were not found in the quantum mechanical cluster calculations due to the limited size and the static nature of calculations. Structurally, there is no intervening water molecule between Na^+ and Cl^- in the H structure.

D. Mechanism of Association/Dissociation Process. The IHS characterization provides structural insight into the Na−Cl ion pair dissociation mechanism. According to our PMF, the TS connecting the CIP and SSIP structures occurs at 3.5 Å. If only the interionic distances are considered, the dissociation process should be initiated by the conversion of R into F_2 groups. The initial step of the dissociation could involve a conversion of IHS from a major R^2 to a minor R^1 type, such as from $R^2{}_1$ to $R^1{}_1R^2{}_1$. The $R^1{}_2$ into F_2 conversion is accompanied by the elongation of interionic distance by about 2.0 Å, which requires a minimal change in the basic IHS structure other than the interionic distance. It suggests that the energy barrier originates from the NaCl bond breakage as well as the solvent reorganization due to the enlarged IHS. Note that the relative population of R^1 and R^2 could also affect the conversion rate from CIP to SSIP. Therefore it would be interesting to study the relation between the transition states and the R^1/R^2 population ratio in other ionic systems. After this major event, the F_2 species are rather easily converted to F_1 by removing one of two "intervening" water molecules or converting one of its F into H. The removal of all F type "intervening" water molecules from the NaCl eventually yields the dissociating ion pair (DIP) of H species. Their populations significantly decrease, as the interionic distance increases beyond 9 Å.

4. CONCLUSIONS

The quantum mechanical cluster calculations and the solution QM/EFP-MD simulations were performed to characterize hydration structures involved in the association/dissociation of NaCl in solution. The QM/EFP-MD simulation provides the accurate free energy profile reproducing CPMD results. In addition to the well-known CIP and SSIP states, the analysis based on our interionic hydration structures (IHSs) established the existence of dissociating ion pair (DIP). The detailed structures of these were well characterized as "ring (R)", "full-bridge (F)", and "half-bridge (H)" types. A strong correlation between the IHSs and interionic distance suggests that not only the solvent reorganization but also the local IHS changes are equally important. In short, our combined QM and QM/EFP-MD study revealed that the ion association process can be well described by the various structural conversions of interionic hydration structure (IHS), providing detailed structural information for the first time. On the basis of our results, we propose a more detailed description of ion dissociation process as

$$\begin{aligned} \underset{\text{ions}}{M^+ + X^-} &\Leftrightarrow M_{\cdots_{DIP(H)}}X \\ &\Leftrightarrow M_{\overset{\cdots}{SSIP(F_1)}}X \\ &\Leftrightarrow M_{\overset{\cdot\cdot}{SSIP(F_2)}}X \\ &\Leftrightarrow M_{\overset{\cdot}{CIP(R)}}X \\ &\Leftrightarrow \underset{\text{salt}}{MX} \end{aligned}$$

■ ASSOCIATED CONTENT

Ⓢ Supporting Information

Figures depicting optimized structures and relative stabilization energies of $NaCl(H_2O)_n$ (n = 1−6) clusters and the calculated radial distribution function for the Na−Cl pair. This material is available free of charge via the Internet at http://pubs.acs.org.

■ AUTHOR INFORMATION

Corresponding Author

*E-mail: sugita@riken.jp, cchoi@knu.ac.kr.

Notes

The authors declare no competing financial interest.

■ ACKNOWLEDGMENTS

This work was supported by a National Research Foundation of Korea (NRF) grant funded by the Korea government (MEST) (No. 2007-0056341, No. 2012-004812, and No. 2012-0002540).

■ REFERENCES

(1) Reichardt, C. *Solvent effects in organic chemistry*; Verlag Chemie: Weiheim, 1979.
(2) Szwarc, M. *Ions and Ion Pairs in Organic Reactions*; Krieger Publishing Co.: Malabar, FL, 1974.
(3) Bountis, T. *Proton transfer in hydrogen-bonded systems*; Plenum Publishing Corp.: New York, 1992.
(4) Ohtaki, H.; Yamatera, H. *Structure and dynamics of solutions*; Elsevier Science Ltd: 1992.
(5) Conway, B. E. *Ionic hydration in chemistry and biophysics*; Elsevier Science Ltd: 1981.
(6) Apse, M. P. *Science* **1999**, *285*, 1256−1258.

(7) Cserháti, T.; Forgács, E. *Int. J. Pharm.* **2003**, *254*, 189−196.
(8) Neysens, P. *Int. J. Food Microbiol.* **2003**, *88*, 29−39.
(9) Rodriguez, P.; Torrecillas, A.; Morales, M.; Ortuno, M.; Sanchezblanco, M. *Environ. Exp. Bot.* **2005**, *53*, 113−123.
(10) Gard, E. E. *Science* **1998**, *279*, 1184−1187.
(11) Oum, K. W. *Science* **1998**, *279*, 74−76.
(12) Knipping, E. M. *Science* **2000**, *288*, 301−306.
(13) Finlayson-Pitts, B. J. *Chem. Rev.* **2003**, *103*, 4801−4822.
(14) Winstein, S.; Clippinger, E.; Fainberg, A. H.; Robinson, G. C. *J. Am. Chem. Soc.* **1954**, *76*, 2597−2598.
(15) Ho, P. C.; Bianchi, H.; Palmer, D. A.; Wood, R. H. *J. Solution Chem.* **2000**, *29*, 217−235.
(16) Ho, P. C.; Palmer, D. A. *J. Chem. Eng. Data* **1998**, *43*, 162−170.
(17) Quist, A. S.; Marshall, W. L. *J. Phys. Chem.* **1969**, *73*, 978−985.
(18) Zimmerman, G. H.; Gruszkiewicz, M. S.; Wood, R. H. *J. Phys. Chem.* **1995**, *99*, 11612−11625.
(19) Oelkers, E. H.; Helgeson, H. C. *Geochim. Cosmochim. Acta* **1991**, *55*, 1235−1251.
(20) Woon, D. E.; Dunning, T. H. J. *J. Am. Chem. Soc.* **1995**, *117*, 1090−1097.
(21) Asada, T.; Nishimoto, K. *Chem. Phys. Lett.* **1995**, *232*, 518−523.
(22) Petersen, C. P.; Gordon, M. S. *J. Phys. Chem. A* **1999**, *103*, 4162−4166.
(23) Jungwirth, P. *J. Phys. Chem. A* **2000**, *104*, 145−148.
(24) Szczęśniak, M. M.; Latajka, Z.; Piecuch, P.; Ratajczak, H.; Orville-Thomas, W. J.; Rao, C. N. R. *Chem. Phys.* **1985**, *94*, 55−63.
(25) Bacelo, D.; Ishikawa, Y. *Chem. Phys. Lett.* **2000**, *319*, 679−686.
(26) Sobolewski, A. L.; Domcke, W. *Phys. Chem. Chem. Phys.* **2005**, *7*, 970−974.
(27) Ault, B. S. *J. Am. Chem. Soc.* **1978**, *100*, 2426−2433.
(28) Kaufmann, E.; Tidor, B.; Schleyer, P. V. R. *J. Comput. Chem.* **1986**, *7*, 334−344.
(29) Olleta, A. C.; Lee, H. M.; Kim, K. S. *J. Chem. Phys.* **2006**, *124*, 024321.
(30) Siu, C.-K.; Fox-Beyer, B. S.; Beyer, M. K.; Bondybey, V. E. *Chem.—Eur. J.* **2006**, *12*, 6382−6392.
(31) Smith, D. E.; Dang, L. X. *J. Chem. Phys.* **1994**, *100*, 3757.
(32) Zhang, Z.; Duan, Z. *Chem. Phys.* **2004**, *297*, 221−233.
(33) Savelyev, A.; Papoian, G. A. *J. Am. Chem. Soc.* **2006**, *128*, 14506−14518.
(34) Savelyev, A.; Papoian, G. A. *J. Am. Chem. Soc.* **2007**, *129*, 6060−6061.
(35) Chen, A. A.; Pappu, R. V. *J. Phys. Chem. B* **2007**, *111*, 11884−11887.
(36) Auffinger, P.; Cheatham, T. E.; Vaiana, A. C. *J. Chem. Theory Comput.* **2007**, *3*, 1851−1859.
(37) Cordomí, A.; Edholm, O.; Perez, J. J. *J. Chem. Theory Comput.* **2009**, *5*, 2125−2134.
(38) Joung, I. S.; Cheatham, T. E. *J. Phys. Chem. B* **2008**, *112*, 9020−9041.
(39) Horinek, D.; Mamatkulov, S. I.; Netz, R. R. *J. Chem. Phys.* **2009**, *130*, 124507.
(40) Kalcher, I.; Dzubiella, J. *J. Chem. Phys.* **2009**, *130*, 134507.
(41) Patra, M.; Karttunen, M. *J. Comput. Chem.* **2004**, *25*, 678−689.
(42) Malani, A.; Ayappa, K. G.; Murad, S. *Chem. Phys. Lett.* **2006**, *431*, 88−93.
(43) Yang, Y.; Meng, S.; Xu, L.; Wang, E.; Gao, S. *Phys. Rev. E* **2005**, *72*, 012602.
(44) Zidi, Z. S. *J. Chem. Phys.* **2005**, *123*, 64309.
(45) Marti, J.; Csajka, F. S. *J. Chem. Phys.* **2000**, *113*, 1154.
(46) Timko, J.; Bucher, D.; Kuyucak, S. *J. Chem. Phys.* **2010**, *132*, 114510.
(47) Masunov, A.; Lazaridis, T. *J. Am. Chem. Soc.* **2003**, *125*, 1722−1730.
(48) Car, R.; Parrinello, M. *Phys. Rev. Lett.* **1985**, *55*, 2471−2474.
(49) Komeiji, Y.; Nakano, T.; Fukuzawa, K.; Ueno, Y.; Inadomi, Y.; Nemoto, T.; Uebayasi, M.; Fedorov, D. G.; Kitaura, K. *Chem. Phys. Lett.* **2003**, *372*, 342−347.
(50) Field, M. J.; Bash, P. A.; Karplus, M. *J. Comput. Chem.* **1990**, *11*, 700−733.
(51) Gordon, M. S.; Fedorov, D. G.; Pruitt, S. R.; Slipchenko, L. V. *Chem. Rev.* **2012**, *112*, 632−672.
(52) Day, P. N.; Jensen, J. H.; Gordon, M. S.; Webb, S. P.; Stevens, W. J.; Krauss, M.; Garmer, D.; Basch, H.; Cohen, D. *J. Chem. Phys.* **1996**, *105*, 1968.
(53) Day, P. N.; Pachter, R.; Gordon, M. S.; Merrill, G. N. *J. Chem. Phys.* **2000**, *112*, 2063.
(54) Netzloff, H. M.; Gordon, M. S. *J. Chem. Phys.* **2004**, *121*, 2711−2714.
(55) Adamovic, I.; Gordon, M. S. *J. Phys. Chem. A* **2005**, *109*, 1629−1636.
(56) Bandyopadhyay, P.; Gordon, M. S. *J. Chem. Phys.* **2000**, *113*, 1104−1109.
(57) Arora, P.; Slipchenko, L. V.; Webb, S. P.; DeFusco, A.; Gordon, M. S. *J. Phys. Chem. A* **2010**, *114*, 6742−6750.
(58) Choi, C. H.; Re, S.; Feig, M.; Sugita, Y. *Chem. Phys. Lett.* **2012**, *539*−*540*, 218−221.
(59) Becke, A. D. *J. Chem. Phys.* **1993**, *98*, 5648−5652.
(60) Lee, C.; Yang, W.; Parr, R. G. *Phys. Rev. B: Condens. Matter* **1988**, *37*, 785−789.
(61) Krishnan, R.; Binkley, J. S.; Seeger, R.; Pople, J. A. *J. Chem. Phys.* **1980**, *72*, 650−654.
(62) Brooks, B. R.; Bruccoleri, R. E.; Olafson, B. D.; States, D. J.; Swaminathan, S.; Karplus, M. *J. Comput. Chem.* **1983**, *4*, 187−217.
(63) Kumar, S.; Rosenberg, J. M.; Bouzida, D.; Swendsen, R. H.; Kollman, P. A. *J. Comput. Chem.* **1995**, *16*, 1339−1350.
(64) Zhu, F.; Hummer, G. *J. Comput. Chem.* **2011**, *33*, 453−465.
(65) Schmidt, M. W.; Baldridge, K. K.; Boatz, J. A.; Elbert, S. T.; Gordon, M. S.; Jensen, J. H.; Koseki, S.; Matsunaga, N.; Nguyen, K. A.; Su, S.; Windus, T. L.; Dupuis, M.; Montgomery, J. A. *J. Comput. Chem.* **1993**, *14*, 1347−1363.
(66) Khavrutskii, I. V.; Dzubiella, J.; McCammon, J. A. *J. Chem. Phys.* **2008**, *128*, 044106.
(67) Stephen, H.; Stephen, T. *Solubilities of inorganic and organic compounds: Binary systems*; Macmillan: New York, 1963; Vol. *1*.
(68) Aragones, J. L.; Sanz, E.; Vega, C. *J. Chem. Phys.* **2012**, *136*, 244508.
(69) Chialvo, A. A.; Cummings, P. T.; Cochran, H. D.; Simonson, J. M.; Mesmer, R. E. *J. Chem. Phys.* **1995**, *103*, 9379.